Joining of Ceramics Demonstrated by the Example of SiC/Ti

B. Gottselig,* E. Gyarmati,‡ A. Naoumidis & H. Nickel

Institut für Reaktorwerkstoffe, Forschungszentrum Jülich GmbH, Postfach 1913, 5170 Jülich, FRG

Abstract

The reaction behaviour of titanium sputtered on silicon carbide was investigated in a series of tests. It was ascertained that, in the temperature range between 1250 and 1500°C, mainly the ternary phase Ti_3SiC_2 is formed (>90%). In joining experiments of silicon carbide with 1–3 µm thick titanium layers at 1450°C at compaction pressures between 5 and 30 MPa the formation of the ternary phase leads to a high joining strength. The achieved bending strength ($\sigma_M \approx 286\,MPa$; $m \approx 10$) is comparable to that of the starting materials ($\sigma_M \approx 303\,MPa$; $m \approx 15$).

Das Reaktionsverhalten von Siliziumcarbid mit aufgesputterten Ti-Schichten wurde in einer systematischen Versuchsreihe untersucht. Es wurde festgestellt, daß im Temperaturbereich zwischen 1250 und 1500°C vorwiegend (>90%) die ternäre Phase Ti_3SiC_2 gebildet wird.
Bei Fügeversuchen von SiC unter Verwendung von Ti-Schichten mit einer 1–3 µm Dicke und Preßdrücken zwischen 5 und 30 MPa bei 1450°C hat die Bildung dieser ternären Phase zu einer hohen Festigkeit des Verbundes geführt. Die erreichte Biegebruchfestigkeit ($\sigma_M \approx 286\,MPa$; $m \approx 10$) ist mit der des verwendeten Ausgangsmaterials ($\sigma_M \approx 303\,MPa$; $m \approx 15$) vergleichbar.

On a effectué une série d'essais portant sur la réactivité de la couche de titane déposée par projection sur le substrat de carbure de silicium. On a constaté qu'entre 1250 et 1500°C, la phase qui se forme majoritairement (>90%) est le composé ternaire Ti_3SiC_2. Sa formation, lors d'expériences réalisées

avec des couches de titane de 1 à 3 µm d'épaisseur à 1450°C sous des pressions comprises entre 5 et 30 MPa, conduit à une résistance élevée de l'interface. La résistance en flexion mesurée ($\sigma_M \approx 286\,MPa$; $m \approx 10$) est comparable à celle des matériaux de départ ($\sigma_M \approx 303\,MPa$; $m \approx 15$).

1 Introduction

Modern engineering ceramics possess significant advantages over metallic materials for a variety of technical applications.[1] Existing disadvantages, such as brittleness and insufficient reproducibility of properties, are being dealt with under current research projects. Furthermore, suitable techniques for joining ceramic materials with each other and with metals are being developed.[2] With regard to the commercial viability of engineering ceramics, there are two main problems. First, the complicated production procedures for producing components out of monolithic pieces should be replaced by simpler, integrated processes. Secondly, techniques are required for the joining of ceramics to metallic components.[3] This area is of critical significance. Brazing,[4,5] diffusion welding[6-8] and those processes in which one of the workpieces involved is fused[9] are suitable for application in the high temperature range which is of particular interest.

Diffusion welding seems to be the most interesting technique for joining ceramics since it may provide basically defined reaction products by means of interlayers ensuring high joint strengths and good temperature stability (Table 1).

Diffusion-welded joints can only achieve their full potential, however, if the reaction process and the reaction layer structure are known and the temperature, time, applied pressure and metal layer thickness

* Present address: Fordwerke AG, John Andrews Entwicklungszentrum, Postfach 604002, 5000 Köln 60, FRG.
‡ To whom correspondence should be addressed.

153

Table 1. Comparative evaluation of joining processes[10]

Requirement criterion	Mech. bond	Adhesive bonding	Brazing	Reaction-welded joints		
				Diffusion welding	Fusion welding	Friction welding
Strength, MPa	10–50	20–80	100–300	100–500	50–200	50–200
Heat resistance	Poor–medium	Poor	Medium–good	Good	Good	Poor–medium
Up to T(K)	700	450	800	1 300	>1 300	500
Tightness	No	Poor	Good	Good	Good	—
Cost	Low–medium	Low	Medium	Medium–high	Low–high	Low–medium
Problems	Stress concentration	—	—	—	Grain growth thermal stress sensitive to thermal shock	Geometry

are optimized. These correlations are only known to date for a few simple systems. More complex systems with several reacting elements have scarcely been examined in the past.

The silicon carbide/titanium system has been extensively studied and will be used here as an example to illustrate in more detail the influences of the above parameters on the joint strength achievable.

2 Experimental

2.1 Materials

Some of the properties of the silicon carbide supplied by ESK are shown in Table 2.

The sintering aids used for this material were aluminium and carbon. Their distribution in the microstructure is not homogeneous. High aluminium concentrations have always been detected in pore regions, whereas high carbon concentrations were found at the grain boundaries.

The titanium used had a purity of >99·0% as confirmed by spectral analysis. The principal impurities were oxygen and iron of 1000 and 400 ppm, respectively.

2.2 Procedures

The relevant process parameters (joining temperature, joining time, applied pressure, metal layer

Table 2. Properties of the SiC material used

SiC	>98·5 wt %
C_{free}	1·0 wt %
Al	0·3 wt %
Si_{free}	—
O, N	traces
SiC modifications	4H, 6H, 15R
Porosity	5·8 ± 1·03 vol. %
Average grain diameter	1·78 × 1·83$^{\pm 1}$ μm

thickness) were studied with regard to the formation of defined reaction products prior to the joining tests on simple layer systems. The results obtained formed the basis for the joining experiments.

In order to determine the reaction products and the reaction kinetics between SiC and a Ti layer, identically processed silicon carbide specimens were first cleaned in an ultrasonic bath. Then the surface impurities were removed by sputtering (etching) with argon ions in a sputtering facility before being coated with titanium with a thickness between 0·2 and 3·0 μm. The specimens were annealed at temperatures between 700 and 1700°C in a resistance-heated high-temperature furnace in argon, using Ti sponge for removing (gettering) the residual oxygen.

The phases formed were studied by means of diffraction analysis using a copper X-ray tube. The X-ray penetrated the complete thickness of films well into the ceramic substrate and supplied information about any unreacted coatings as well as about the phases formed. The evaluation of the X-ray diffractometer patterns permits statements to be made about the relative fractions of the reaction products arising as a function of the annealing parameters, but not on their absolute fractions. Nevertheless, qualitative statements on the reaction process are possible. For this purpose, three peaks were selected from each of the phases identified, their integrated intensities were summed and related to the total intensity calculated from the sum of the integrated intensities of all phases considered. It turned out to be necessary to select three peaks since a preferred orientation in the metal layer had been detected in preliminary tests. The respective peaks of the individual phases were selected according to the following criteria:

—Their position within the angular range $20° < 2\theta < 60°$;

—they are available for all experiments;

—they will not coincide with reflections of other phases;

—they should exhibit the highest possible intensities.

This procedure made it possible to describe the reaction process in terms of relative fractions of phases over the annealing temperature.

The specimen surface was additionally examined by means of Rutherford backscattering and Auger spectroscopy. Ceramographic cross-sections were studied by optical and scanning electron microscopy and electron probe microanalysis to determine the phase distribution in the reaction zone. The adhesion of the reaction layers on the substrate was examined by a scratch test.

The process parameter combinations found to be suitable as a result of these investigations were then used for joining experiments. The joint strength of the specimens was tested in four-point bend tests with standard dimensions $w \times h \times l = 4.5 \times 3.5 \times 50$ mm. The process for preparing the four-point bend test specimens is shown schematically in Fig. 1.

The surface roughness, R_a, of the bend test pieces was 0.05μm. The cross-head speed was for all tests 0.25 mm/min. The test atmosphere was laboratory air at 23°C. The standard specimens were also produced according to the above procedure. Prior to testing, some of the standard specimens were exposed for 60 min to an Ar/H_2 atmosphere at 1400°C, others were tested without exposure. Both standard specimen series did not reveal any significant differences in strength behaviour.

3 Results and Discussion

3.1 Reaction mechanism and kinetics

After coating the SiC specimens with Ti, no phase formation was detected at the interface by either Rutherford backscattering (RBS) or X-ray diffractometry.

Three temperature ranges have been established with respect to the phases formed after an annealing time of 2 h:

—700–1200°C: Formation of a substoichiometric titanium carbide layer in direct contact with SiC and diffusion controlled formation of different titanium silicides on TiC has been observed. The formation of the individual titanium silicides is dependent on the unreacted titanium available.

—1200–1500°C: Complex carbide Ti_3SiC_2 is formed predominantly. The fraction of this phase within the total reaction product amounts to $>90\%$. Other reaction phases in this temperature range (TiC, $TiSi_2$) form fractions below 5%.

—1500–1700°C: Titanium carbide, i.e. the thermodynamically most stable phase of the Ti–Si–C system, is the end product of the reaction after evaporation of the silicon present in the intermediate reaction products.

The phase fractions of the individual phases are plotted in Fig. 2 over the annealing temperature.

The results of X-ray diffraction analysis do not provide information about the layer sequence in the reaction phase. The layer structure was elucidated by means of electron probe microanalysis on cross-sections. The first reaction phase (titanium carbide) was detected in direct contact with the ceramic before the diffusion-controlled formation of titanium silicides takes place in the layer above this phase. If a sufficient amount of unreacted titanium is available for this reaction, congruently melting titanium silicide (Ti_5Si_3) with isolated islands of titanium carbide is formed above the titanium carbide layer. The further reaction process is then determined by the stability of the individual reaction

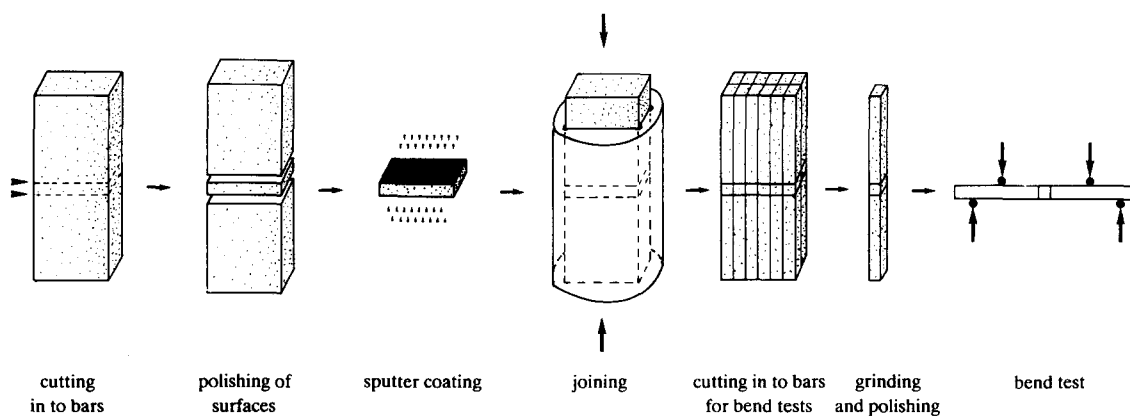| cutting into bars | polishing of surfaces | sputter coating | joining | cutting in to bars for bend tests | grinding and polishing | bend test |

Fig. 1. Schematic diagram of the preparation of bend test specimens from joined SiC prisms.
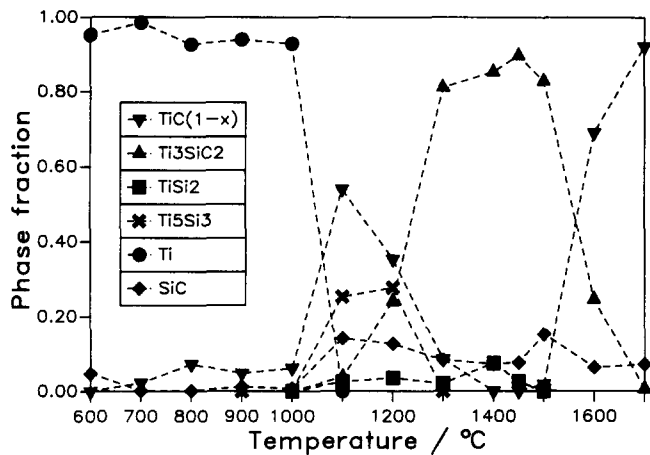
Fig. 2. Fractions of phases formed during the reaction between SiC and a 3 μm thick titanium layer after annealing for 2 h at different temperatures.

phases with respect to each other. The ternary phase Ti_3SiC_2 is formed in direct contact with the ceramic, partially involving a reaction of the titanium carbide with the SiC and leading to a shift in the layer sequence described above (Fig. 3).

At 1450°C the reaction layer is only composed of the ternary phase and small fractions of $TiSi_2$ which, however, cannot be localized by microprobe techniques. The reaction layer structure is schematically shown in Fig. 4 for the four temperature ranges.

Increasing annealing times beyond 2 h leads to a layer sequence corresponding to a heat treatment at temperatures about 100°C higher. An influence of the layer thicknesses on the reaction process was not observed. An evaluation of layer thickness growth shows a parabolic dependence on time. The correlation coefficients, R, of this dependence were in the range of $R > 0·97$ for all temperature levels so that a parabolic and thus diffusion-controlled time law can be assumed which is described by the equation
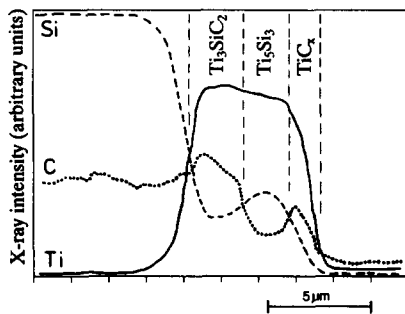
$$2k = 2k_0 \exp(-Q/RT)$$

Fig. 3. Line-scan through the reaction layer of a specimen after annealing at 1200°C for 2 h to identify the structure of the reaction layer. The layer sequence is as follows: $SiC–Ti_3SiC_2–(Ti_5Si_3 + TiC)$.
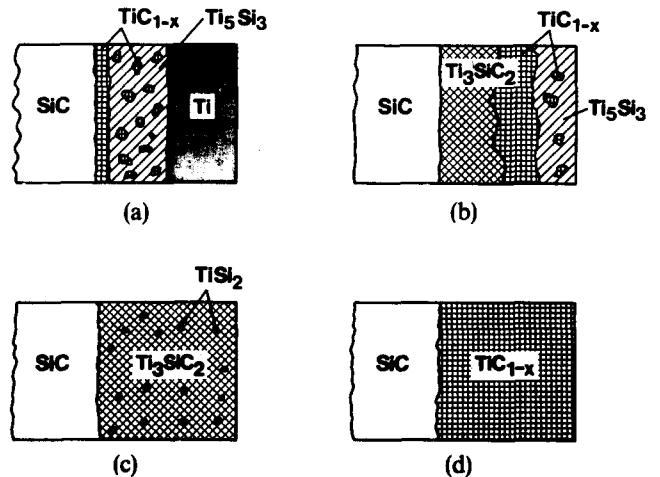

Fig. 4. Schematic structure of the reaction layer (after annealing for 2 h) of a 3 μm Ti layer on silicon carbide at (a) $T < 1000°C$, (b) $1000°C < T < 1250°C$, (c) $1250°C < T < 1500°C$ and (d) $T > 1500°C$.

The term

$$2k = \frac{x^2}{t}$$

was determined by measuring the reaction layer thickness (x). The activation energy of the reaction thus obtained $(Q = 311 \text{ kJ/mol}$ and the frequency factor $2k_0 = 65 \text{ cm}^2/\text{s})$ differs in part significantly from the literature values[11–14] (Fig. 5). The deviations ascertained are presumably attributable, however, to different carbon or silicon concentrations or to different SiC modifications (α- or β-SiC). A generalization of reaction constants is not possible.

3.2 Joining tests

The use of a thin metal film for joining two ceramic parts requires exact knowledge of the reaction products formed as a function of temperature and of
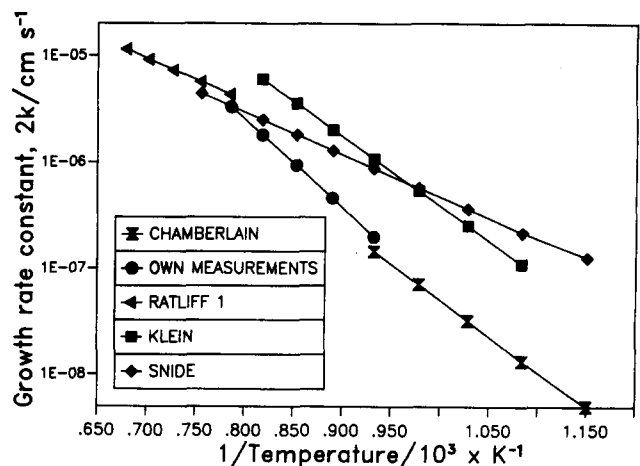

Fig. 5. Comparison of the reaction constants determined in this work with literature data.[11–14]

a number of further factors of significance for achieving high joint strengths, such as:

—The physical and chemical properties of the reaction products;

—the long-time stability of the reaction phases;

—lattice coherence between reaction phase and ceramics;

—adhesion between the two materials;

—possible weakening of the composite material in the joint by pore formation during the reaction between ceramics and metal.

The properties of the individual reaction phases are not completely known for the application of Ti films on SiC. As regards their mechanical properties, the joints between titanium and carbon or silicon are mostly very brittle.[15] Exceptions are titanium carbide, due to its metallic structure, and the ternary phase Ti_3SiC_2. Plastic behaviour was definitely observed for the latter phase produced in the Chemical Vapour Deposition (CVD) process.[16]

Moreover, coherent phase boundaries have been found between SiC and the ternary phase due to good agreement of the lattice parameters. This leads to very good adhesion of the ternary phase on the ceramics, as is also shown by the results of scratch testing (Fig. 6(a)–(d)).[17]

Insufficient ductility of the reaction phase, poor agreement of the lattice parameters and complex reaction layers (several phases with very different properties) are the cause for low adhesive strengths (low critical load) as shown in Fig. 6(a) and (b). Specimens under the conditions shown in Fig. 6(c) and (d) only differ slightly with respect to the critical load determined.

In view of the results obtained from these tests, the ternary phase (Ti_3SiC_2) appears particularly suitable for the formation of an interlayer for joining SiC with itself. In order to verify this assumption, joining tests were carried out involving the selective production of the ternary phase.[16] Table 3 contains the parameters of some of the experiments carried out.
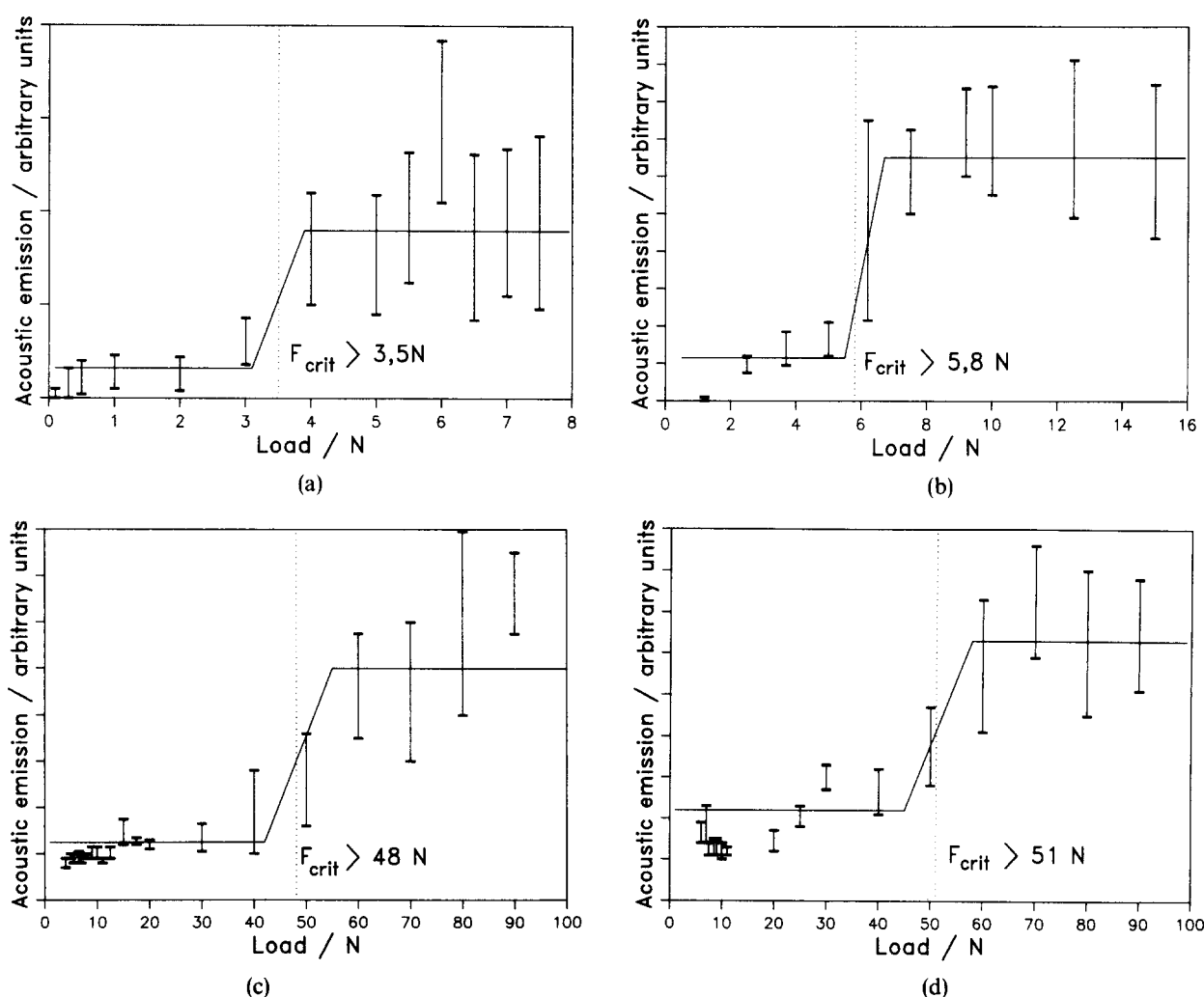

Fig. 6. Comparison of acoustic emission data determined during scratch tests on different reaction layers formed in the interaction between a 3 μm thick Ti layer and SiC. Conditions and layers: (a) 700°C/2 h, $TiC_{0.45}$; (b) 1100°C/2 h, Ti_3SiC_2 + $TiC_{0.45}$ + Ti_5Si_3 + $TiSi_2$; (c) 1450°C/2 h, Ti_3SiC_2; (d) 1600°C/2 h, $TiC_{0.8}$.

Table 3. Process conditions for joining SiC materials with the aid of Ti interlayer

Parameters	Test numbers			
	(1)	(2)	(3)	(4)
Roughness of the matching surfaces, R_a, μm	0·05	0·05	0·05	0·05
Titanium layer thickness, μm	1·0	1·0	3·0	3·0
Heating rate, K/min	300	300	150	300
Joining temperature, °C	1450	1450	1450	1450
Joining time, h	1·0	1·0	0·5	1·0
Joining pressure, MPa	30	5	15	30

Atmosphere of hot press equipment: Ar/4% H_2.

The joint strengths determined in the four-point bend test for the specimens of test (1), (3) and (4) are within the strength range of the starting material. The fracture position for 70% of the specimens is in the ceramics and not in the joint. Test (2) generally shows the fracture position to be within the joint. In order to compare the strength behaviour of joined specimens with the ceramic starting material ($\sigma_M \approx 303$ MPa; m ≈ 15), strength values were plotted in a double-logarithmic Weibull plot (Fig. 7).

An evaluation according to Weibull is, strictly speaking, only acceptable for unjoined specimens. The m and σ_M values specified for the joined specimens do not meet the requirements of an isotropic material structure. They can, therefore, be used exclusively for a relative evaluation and not in the sense of the Weibull theory, e.g. for describing the size effect.

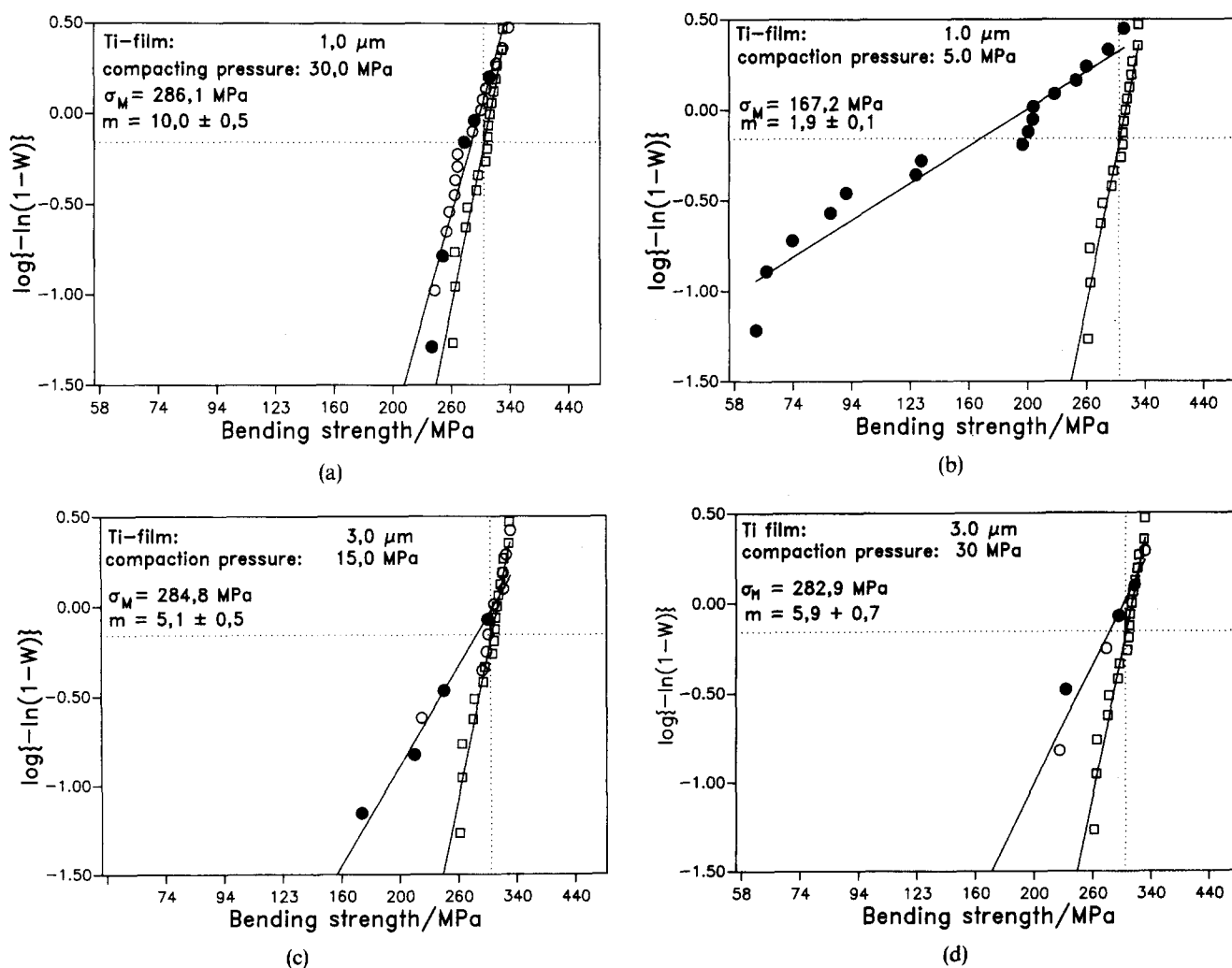The ternary phase in the interlayer responsible for the strength level achieved was detected both by X-

Fig. 7. Weibull plot of the joint strength of four test series. ○, fracture in the ceramics; ●, fracture in the joint; □, measured values of the starting material. (a) Test 1; (b) test 2; (c) test 3; (d) test 4.
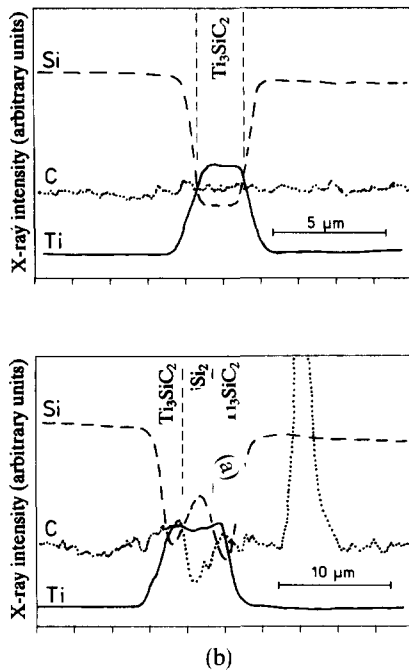
Fig. 8. Line scans for Ti, Si, C across the joint of specimens joined with a titanium layer (a) 1·0 μm and (b) 3·0 μm thick.

ray diffraction and microprobe analysis. It was found that the 1·0-μm thick titanium layers react to form homogeneous films during the joining process. Using 3·0-μm thick titanium layers a continuous layer of $TiSi_2$ was detected in the centre of the Ti_3SiC_2 layer (Fig. 8).

Both tests (1) and (4) were joined at 30 MPa. The line scan profile in Fig. 8(a) corresponds to a specimen with a strength of $\sigma_M = 301$ MPa, that in Fig. 8(b) to a specimen with a strength of 233 MPa. The strength level of specimens with a continuous $TiSi_2$ layer is always below that of specimens without this additional interlayer. The brittleness of this phase constitutes the weak point determining the strength in the joint. It leads to fracture in the joint and thus to a deterioration of the strength level and to lower *m* values in comparison with test (1). This behaviour can be identified macroscopically by minor spallations in the joint. Microscopic analysis shows that these regions had been filled by the $TiSi_2$ phase prior to strength testing.

The formation of the $TiSi_2$ layer at a given temperature depends mainly on the original thickness of the titanium and on the duration. For short durations and thin titanium layers, the $TiSi_2$ forms a fine dispersion. For longer durations, agglomeration of $TiSi_2$ takes place. If thick titanium layers are used, similar processes again occur but the agglomeration leads to the formation of a $TiSi_2$ intermediate layer.

Joining pressures beyond 10 MPa lead to very good contact of the surfaces to be joined. The ternary phase enables pores of the ceramics to be
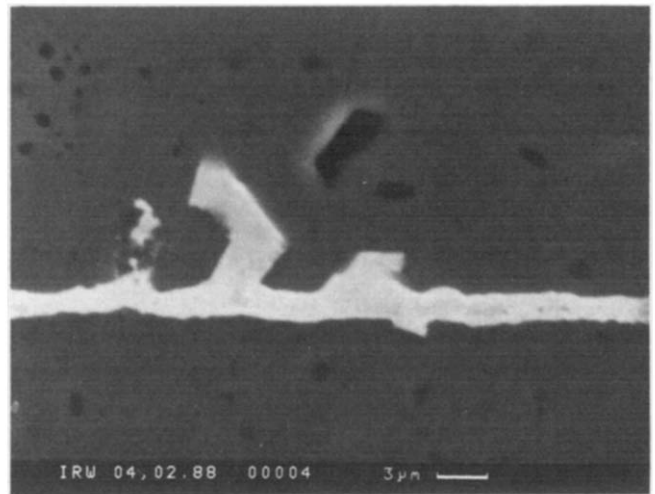

Fig. 9. Pores of the ceramic base material filled with Ti_3SiC_2 in the region of the joint.

filled (Fig. 9). This enlargement of the contact surface beyond the geometrical surface increases the mechanical keying of the joint and as a result the stress-bearing capacity is higher. Joining pressures below 10 MPa do not lead to a good contact between SiC and the ternary phase during the joining process (test (2)). The joint strengths achievable are therefore below the values of the other two tests, as illustrated by the median value of strength and also by the Weibull modulus. All bend tests showed fracture to be within the joint.

The strength behaviour can therefore only be further optimized with the aid of the layer thickness and joining pressure. Although shorter joining times are possible at higher joining temperatures at which pure titanium carbide is formed ($T > 1600°C$), the strength level thus achievable is clearly below the strengths achievable through Ti_3SiC_2 layers.[18] The fracture plane is always in the joint.

4 Conclusions

Experiments on simple layer structures served to clarify the reaction behaviour of titanium with silicon carbide and to derive suitable joining conditions. The possibility of selectively forming ternary phase Ti_3SiC_2 with its specific properties appears particularly interesting with a view to high joint strengths.

Joining with the aid of this phase may lead to joint strengths comparable to the strength of the bulk ceramic material. SiC joints using reaction layers of Ti_3SiC_2 can produce reliable and resistant joints due to their high strength level so as to eliminate weak points under load.

Acknowledgements

References

1. Salmang, H. & Scholze, H., *Keramik, Teil I.* Springer-Verlag, Berlin, 1982.
2. Ziegler, G., Keramische Konstruktionswerkstoffe—Stand der Technik. In *VDI-Tagung*, Essen, April 1987, pp. 1–19.
3. Willmann, G., Randbedingungen für die konstruktive Gestaltung von keramischen Bauteilen. Keram. Z., **36**(12) (1984) 669–673.
4. Iwamoto, N., Umesaki, N., Kamai, M., Katayama, Y., Kawamura, H., Yamamuro, H. & Krozumi, Y., Reaction and compatibility of molten filler alloys with superalloys and silicon nitride. In *Proc. 5th Int. Conf. on High Technology Joining*, BABS, Brighton, 1987, pp.
5. Lugscheider, E., Boretius, M., Grellner, W. & Krappitz, H., The joining of silicon carbide to metals by active brazing. In *Proc. 5th Int. Conf. on High Technology Joining*, BABS, Brighton, 24/1, 1987, pp.
6. Suganuma, K., Okamoto, T., Koizumi, M., Fujita, T. & Miihara, K., Joining of Si_3N_4 with metallic interlayers. In *Proc. 5th Int. Conf. on High Technology Joining*, BABS, Brighton, 1987.
7. Naka, M., Saito, T. & Okamoto, I., Niobium silicides at interface between niobium and SiC. *J. Mat. Sci. Lett.*, **6** (1987) 875–6.
8. Rhodes, C. G., Ghosh, A. K. & Sperling, R. A., Ti–6Al–4V–2Ni as a matrix material for a SiC-reinforced composite. *Metall. Trans. A*, **18A** (12) (1987) 2151–6.
9. Popper, P., The joining of industrial ceramics to metals. In *Proc. 4th Int. Meeting on Modern Ceramics Technologies, Mat. Sci. Monographs 6*, Saint-Vincent, Italy, May 1979, ed. P. Vincenzini. Elsevier, Amsterdam, The Netherlands, 1980, pp. 569–81.
10. Suganuma, K., Miyamoto, Y. & Koizumi, M., Joining of ceramics and metals. *Ann. Rev. Mat. Sci.*, **18** (1988) 47–73.
11. Broutman, L. J. & Krock, R. H. In *Composite Materials, Vol. 1: Interfaces in Metal Matrix Composites*, ed. A. G. Metcalfe. Academic Press, London, New York, 1974, pp. 65–123.
12. Chamberlain, M. B., Solid state reaction of titanium and (0001)α-SiC. *Thin Solid Films*, **72**(2) (1980) 305–11.
13. Ratcliff, J. L. & Powell, G. W., Research on diffusion in multiphase ternary systems. AFML-TR-70-42, Air Force Systems Command, Wright–Patterson Air Force base, Ohio, 1970.
14. Snide, J. A., Ashdown, F. A. & Myers, J. R., High temperature compatibility between vapour-deposited SiC filaments and titanium. *Fiber Sci. Techn.*, **5** (1972) 61–83.
15. Maliszewski, I., Gyarmati, E., Grübmeier, H., Lison, R. & Naoumidis, A., Ein Beitrag zur Verbindung von SiC-Keramiken. In *Proc. Int. Tagung Fügen von Keramik, Glas und Metall*, Vol. 1, No. 2, Bad Nauheim, March 1985, Fortschrittsberichte der DKG, pp. 188–98.
16. Jeitschko, W. & Nowotny, H., Die Kristallstruktur von Ti_3SiC_2—ein neuer Komplexcarbid-Typ. *Monatshefte Chemie*, **98** (1967) 329–37.
17. Gottselig, B., Gyarmati, E., Naoumidis, A. & Nickel, H., Beitrag zur Verbindungstechnik von SiC-Keramik über metallische Zwischenschichten. Report of KFA-Jülich, Jül-2288 (1989), pp. 1–177.
18. Gyarmati, E., Kesternich, W. & Förthmann, R., Fügen von Siliciumcarbid mit Hilfe dünner Ti-Schichten. *Ceram. Forum Int., Ber. DKG*, **66**(7/8) (1989) 292–7.